JACS
JOURNAL OF THE AMERICAN CHEMICAL SOCIETY

Subscriber access provided by ST FRANCIS XAVIER UNIV

Perspective

Monolithic 3D Cross-linked Polymeric Graphene Materials and the Likes: Preparation and Their Redox Catalytic Applications

Yanhong Lu, Yanfeng Ma, Tengfei Zhang, Yang Yang, Lei Wei, and Yongsheng Chen

J. Am. Chem. Soc., **Just Accepted Manuscript** • DOI: 10.1021/jacs.8b06414 • Publication Date (Web): 13 Aug 2018

Downloaded from http://pubs.acs.org on August 13, 2018

Just Accepted

"Just Accepted" manuscripts have been peer-reviewed and accepted for publication. They are posted online prior to technical editing, formatting for publication and author proofing. The American Chemical Society provides "Just Accepted" as a service to the research community to expedite the dissemination of scientific material as soon as possible after acceptance. "Just Accepted" manuscripts appear in full in PDF format accompanied by an HTML abstract. "Just Accepted" manuscripts have been fully peer reviewed, but should not be considered the official version of record. They are citable by the Digital Object Identifier (DOI®). "Just Accepted" is an optional service offered to authors. Therefore, the "Just Accepted" Web site may not include all articles that will be published in the journal. After a manuscript is technically edited and formatted, it will be removed from the "Just Accepted" Web site and published as an ASAP article. Note that technical editing may introduce minor changes to the manuscript text and/or graphics which could affect content, and all legal disclaimers and ethical guidelines that apply to the journal pertain. ACS cannot be held responsible for errors or consequences arising from the use of information contained in these "Just Accepted" manuscripts.

ACS Publications

is published by the American Chemical Society. 1155 Sixteenth Street N.W., Washington, DC 20036

Published by American Chemical Society. Copyright © American Chemical Society. However, no copyright claim is made to original U.S. Government works, or works produced by employees of any Commonwealth realm Crown government in the course of their duties.

Monolithic 3D Cross-linked Polymeric Graphene Materials and the Likes: Preparation and Their Redox Catalytic Applications

Yanhong Lu,[*,†] Yanfeng Ma,[‡] Tengfei Zhang,[‡] Yang Yang,[‡] Lei Wei,[†] and Yongsheng Chen[*,‡]

[†]School of Chemistry & Material Science, Langfang Normal University, Langfang 065000, China

[‡]Centre of Nanoscale Science and Technology and Key Laboratory of Functional Polymer Materials, College of Chemistry, Nankai University, Tianjin 300071, China

E-mail: yschen99@nankai.edu.cn; yanhonglu@mail.nankai.edu.cn

ABSTRACT

While there have been tremendous studies about graphene and its applications in the last decade, so far the proposed huge potential of this material has not been materialized. One of the prerequisites to overcome these challenges is maintaining the nature and intrinsic properties of individual graphene sheets while in the state of bulk material. Thus, in this perspective contribution, the fabrication/synthesis of the monolithic polymeric and three-dimensional (3D) cross-linked bulk materials (3DGraphene) with (doped) 2D graphene sheets as the building block will first be briefly summarized. Then, the second part will cover the redox catalytic application of

these bulk materials including doped 3DGraphene, the graphene-like material polymeric C_3N_4 and their hybrid materials. These will include mainly oxygen reduction reactions (ORR), hydrogen evolution reactions (HER) and CO_2 reduction for their latest development. Finally, challenges and future perspectives related to the design of 3D cross-linked graphene based materials and their catalytic applications will be briefly discussed.

INTRODUCTION

Currently, the most challenging issue for truly large scale applications of graphene is preparing this material in bulk state, while simultaneously maintaining its unique two-dimensional (2D) structure, thus keeping its many excellent properties[1,2] as it has been well known that perfect 2D graphene cannot exist in the free state.[3] While this appears obvious and straight forward, it has yet to be fully realized and has been hampered mainly by the strong and intrinsic intention of restacking of graphene sheets due to strong π-π interactions between the sheets.[4] In fact, most, if not all, reported graphene bulk materials so far have such issues,[5] and many of the wonderful properties of graphene have only been partially utilized in the bulk state.[6,7] Clearly, these reported materials only show incremental/partial utilization of graphene's properties and miss the huge potential for some truly killer application widely expected.[8] In this content, the bulk state and monolithic materials with some types of three-dimensional (3D) cross-linked graphene (3DGraphene) structures become the

choice, where the graphene sheets must be separated in the direction (*c*-axis, out of plane) perpendicular to the graphene basal plane, and better further locked to overcome the intrinsic π-π interaction forces and achieve macroscopic structural stability.[3, 9,10]

One effective strategy, but with some sacrifice, to achieve such 3DGraphene materials is to engineer a graphene material in which individual graphene sheets are bonded together at the edges with C-X bonds (X, = C, O, S, etc, and even some molecules).[4,11] In the proposed 3DGraphene materials to be covered in this work, graphene sheets are kept separated in the *c* axis because of the chemical linkages at the edges and are also locked to have bulk structural integrity stability for the materials.[12,13] Thus, in principle these bulk materials should exhibit intrinsic graphene properties at macroscopic scale. The combination of graphene properties and the material's structural stability should ensure their exciting in electronics, optical, catalytic, mechanical devices (units) and other applications.[14-17]

On the other side, among many proposed possible applications of graphene materials, one of the focuses has been on using this carbon-only material for catalytic applications.[18-20] One of the driving forces in this push is due to the issues of current state-of-art catalysts used in industry. One of such issues is that many of the most popular and efficient industrial catalysts are noble metal based materials, resulting in high costs and other issues.[21,22] Thus, recently an increasing thrust has been emerging to develop metal-free or even carbon-only catalysts with the advantages of different

morphologies, doping and an easily tunable molecular structure as a cost-effective alternative for various photo-/electro- catalytic reactions. As a typical 2D nanocarbon material, graphene based materials have attracted much attention due to its many unique and excellent properties, including its large surface area, efficient light absorption, large π conjugation system and high charge mobility, and chemical stability, all beneficial for high catalytic activity.[23,24] As has been mentioned above, 3DGraphene materials including heteroatom doped ones, could utilize better the advantages of graphene's many intrinsic properties at bulk state and thus are expected to demonstrate superior catalytic activity.[25-27]

Thus, in this perspective, we will first briefly summarize the synthesis and fabrication of these chemically cross-linked 3DGraphene materials with/out doping in bulk state, as this is the starting point for any further studies and serious applications. This include two main parts: 1) template directed methods, including chemical vapor deposition (CVD) growth and solution based template method, 2) the wet chemistry method from graphene oxide (GO) through cross coupling in solution.

Currently, probably due to the extreme importance of redox catalytic reactions and also the matching features of graphene materials, the most studied and also important catalytic reactions using these 3D cross-linked graphene materials are oxygen reduction reactions (ORR), hydrogen evolution reactions (HER) and CO_2 reduction. Thus, these types of catalytic reactions with 3DGraphene materials will be discussed, where at least some intrinsic properties of individual graphene sheets have

been utilized, particularly at the bulk state. To be complete and also for comparison, normal cross-linked 3DGraphene materials with/out doping, graphene like polymeric C_3N_4 and their hybrids will be covered. Final notes will be given for the outlook and challenges in terms of both the preparation and catalytic applications for these materials, where much more attention is required to further control the morphology, active sites, and better understand the catalytic mechanism to prompt the truly possible application of these wonderful materials.

FABRICATION AND PREPARATION OF 3DGRAPHENE

Even before and also after the emerging of graphene studies, there have been many theoretical proposals and studies about such 3DGraphene polymeric structures.[28-30] Importantly, in addition to the unique electronic and mechanical properties derived from graphene,[31,32] most of these proposed graphene based networks, including that with sp^2-sp^3 hybridized structures, are thought to be highly stable. While the ordered (crystalline) 3DGraphene materials have not been proved/prepared completely, some materials with the proposed network structures but in the amorphous form have been reported, and indeed they demonstrate many excellent and unique properties.[12,16,33-35]

Regarding to the synthesis/fabrication, there are mainly two types of approaches to achieve such 3DGraphene materials, as shown in Scheme 1. One is to use

conventional CVD growth or solution assembly with some types of 3D network templates, where the graphene network grows directly on such 3D templates. The other one is based on the wet chemistry approach without a template, using graphene oxide (GO) sheets directly and then cross-linking them together either with themselves or some linking agents. These two approaches will be summarized and discussed separately in the following sections.

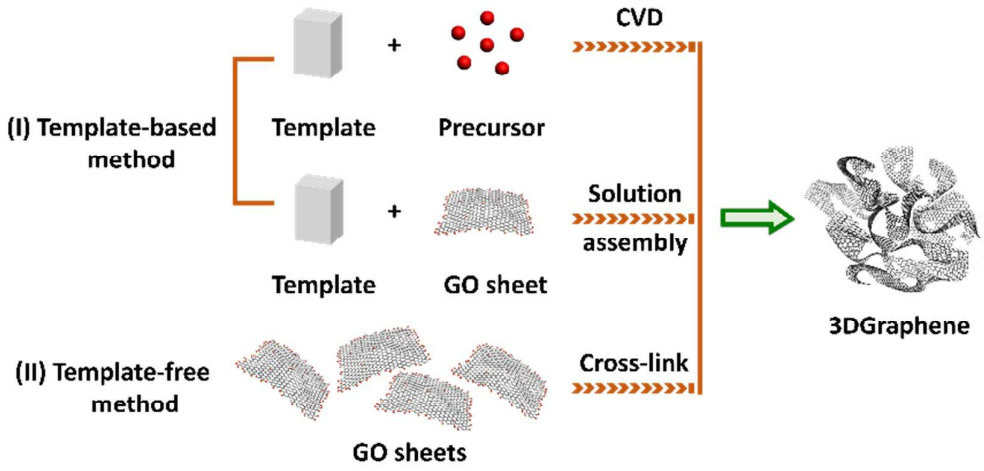

Scheme 1. The schematic of two typical synthetic methods of 3DGraphene materials. (I) The template-based method, including CVD growth or solution assembly protocol. (II) The template-free method using the wet chemistry approach by cross-linking of GO sheets.

CVD GROWTH OR SOLUTION ASSEMBLY ON 3D TEMPLATE FOR 3DGRAPHENE MATERIALS

While almost all CVD approaches use some types of 3D templates, there is at least one exception coming from the excellent work of the Krainyukova group.[36] Using a modified arc approach (but without arc discharge) where only carbon sublimation in vacuum is allowed, a very stable honeycomb carbon allotrope was obtained. High resolution TEM and other analysis results indicate that this material consists of both periodic and random Y-junction type repeating units with a honeycomb structure built exclusively from sp^2-bonded carbon atoms as shown in Figure 1, and is considered as a truly 3DGraphene. This foam material, with an estimated density of ~1.48 g/cm^3, demonstrates high levels of physical absorption of various gases unattainable in other carbon forms such as fullerenes or nanotubes.

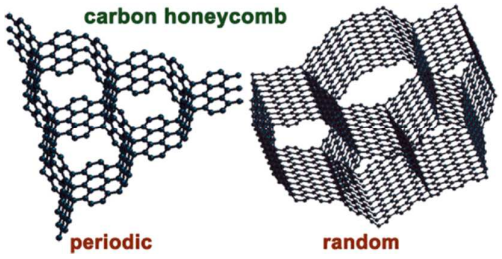

Figure 1. The proposed periodic and random honeycomb carbon structures prepared by a modified arc method from carbon rod directly. Reproduced with permission from ref 36. Copyright 2016, American Physical Society.

Using various pre-fabricated/defined 3D templates and CVD growth on such 3D templates, graphene foams (GF) have been fabricated by different groups. The first

and probably most important work comes from Cheng's group in 2011,[34] where a monolith of a continuous and interconnected foam-like graphene 3D network was obtained using the pre-defined 3D Ni foam template by a direct CVD growth with CH_4 as the carbon source (Figure 2A). After the growth, Ni was etched off and a free-standing GF was obtained which inherits the interconnected 3D scaffold structure of the nickel foam template. All the graphene sheets in the GF are directly bonded each other, resulting in an interconnected and monolithic flexible network of graphene. The free-standing GF is extremely light (~ 2 - 3 mg/cm^3) and flexible, along with a very high specific surface area (up to 850 m^2/g) and electrical conductivity. Similar work was soon reported afterwards by Ruoff's group but with a different etchant.[37] With the input of N, B precursors to the carbon source and following a similar approach, N,B co-doped 3D GFs could also be made in the same way.[38] In 2012, Polsky's group started with an amorphous carbon structure prepared by lithographically predefined 3D pyrolyzed photoresist films, and after conformably sputtering Ni on such predefined 3D carbon structure then followed by annealing and acidic etching off the nickel, a well-defined 3D porous and multilayered graphene network could be prepared.[39] Cyclic voltammograms using this material as the electrode indicate that this material exhibits more favorable electron transfer kinetics than conventional glassy carbon. Yoon *et al*. in 2013 reported an approach to synthesize CVD-grown 3DGraphene nano-networks (3D-GNs) that can be mass produced with large-area coverage for any arbitrary shape and on any electronic device-compatible substrate, such as Al_2O_3, Si, GaN, or Quartz.[40] The procedure

(Figure 2B) consists of four steps, with an annealing step of a PVA/iron precursor infiltrated into 3D-assembled-colloidal silica under a hydrogen environment. This reduces iron ions and generates few-layer graphene by precipitation of carbon on the iron surface and allowing the 3D-GN to be grown. Afterwards the iron/SiO_2 could be removed with HF/HCl solution, leaving few-layer 3D-GN structures on the SiO_2/Si substrate. The produced 3D-GN exhibits a high conductivity of 52 S/cm and high surface area of 1,025 m^2/g.

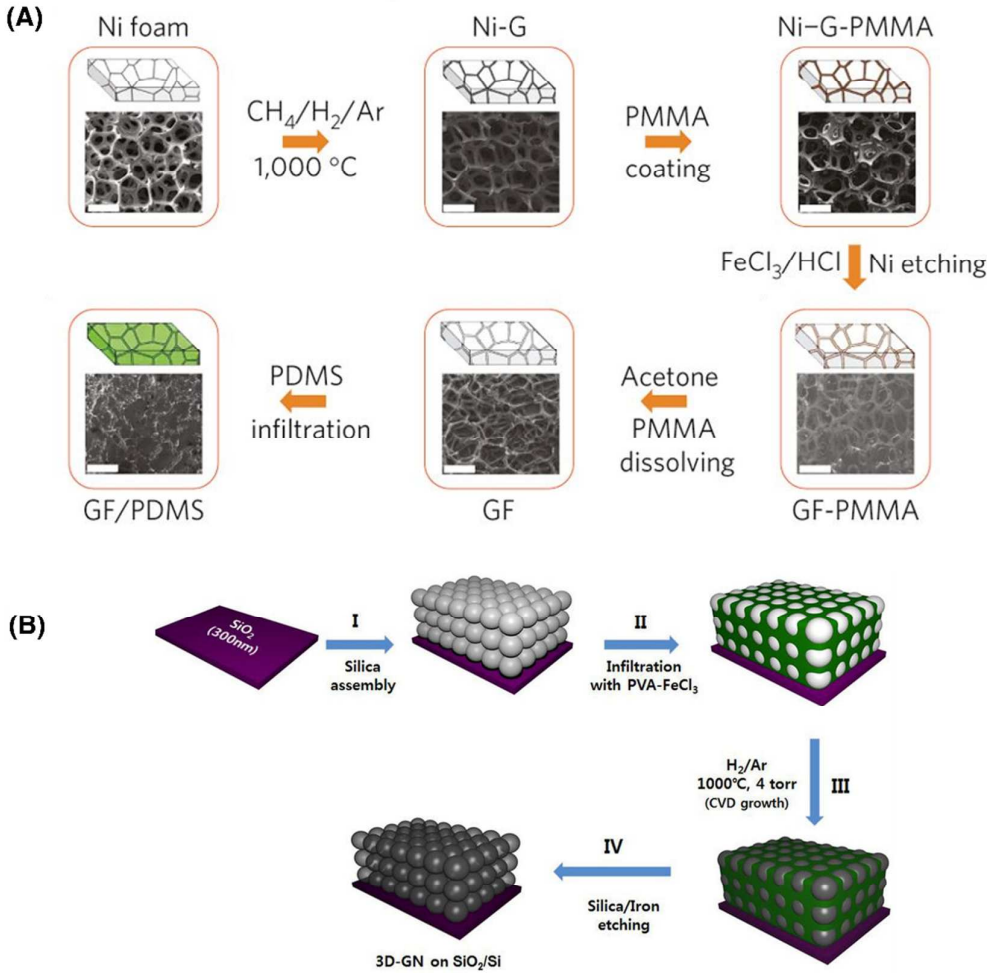

Figure 2. (A) Synthesis of a GF and integration with PDMS. All the scale bars are 500 μm. Reproduced with permission from ref 34. Copyright 2011, Nature Publishing Group. (B) Schematic illustration of the fabrication process for a 3D-GN. Reproduced with permission from ref 40. Copyright 2013, Nature Publishing Group.

In 2013, Shen's group started with a macroporous acrylic-type resin as the carbon precursor with infiltrated Ni catalyst precursor and KOH activator, followed by heating treatment at 850 ℃ and HCl solution washing, a 3D hierarchical porous graphene-like (3D HPG) material was prepared (Figure 3A).[41] Structural and spectrum analysis confirms that the material consists of an interconnected 3D porous graphene network, arising from the thin walls of a few layers of graphene sheets. The material exhibits high surface area up to 1810 m^2/g, total pore volume of 1.22 cm^3/g and high supercapacitor performance when used as the active materials. Using a H-type zeolite as the template and a direct CVD growth followed by HF washing of the zeolite (Figure 3B),[35] a cross-linked-fullerene-like framework, containing carbon hexagons and pentagons with all sp^2 carbon, was obtained, and the building unit of the carbon framework in each supercage of the zeolite Y has an average composition of $C_{63}H_{4.9}O_{1.2}$, very close to that of fullerene C60 cross-linked-fullerene-like framework Schwarzite carbon structure.[30] It also exhibits a typical semimetal band structure with zero bandgap.

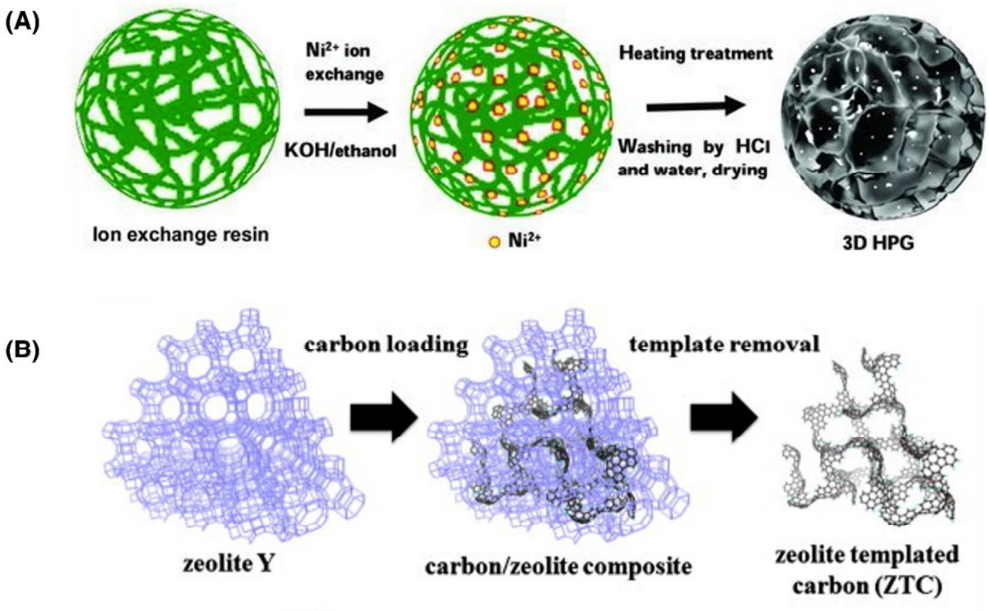

Figure 3. (A) The synthetic steps of 3D HPG. Reproduced with permission from ref 41. Copyright 2013, Wiley-VCH. (B) Synthetic scheme for conventional ZTC consisting of a cross-linked-buckybowl-like framework. Reproduced with permission from ref 35. Copyright 2013, Elsevier.

Recently, a very interesting and unique approach was developed by Chen's group to prepare free-standing and high quality 3DGraphene networks.[33] The procedure started by chemically echoing out Mn in a $Ni_{30}Mn_{70}$ alloy to first generate a nanoporous Ni foam film, followed by a CVD process under a mixed atmosphere of H_2, Ar, and benzene. The free-standing complex 3D network comprised of interconnected graphene was then obtained by chemically removing the nanoporous Ni substrate in HCl solution. Importantly, the obtained free standing film retains many intrinsic properties of individual graphene sheets, including the basic electronic

properties of graphene, indicating the high quality of the graphene units in the structure and its potential for the practical application of graphene in 3D devices in the future.[33] In 2016, Wu and co-workers developed an ambient-pressure CVD method followed by post-doping with a solid nitrogen rich precursor graphitic-C_3N_4 to prepare a N-doped 3DGraphene foam.[42] The 3DGraphene foam incorporated with nitrogen defects as a metal-free catalyst for CO_2 reduction shows excellent activities, and this will be discussed more in next section.

Besides CVD growth, solution templates have also be widely used to construct 3DGraphene materials through the assembly of GO sheets onto 3D templates followed by chemical reduction process. Several typical templates, such as silica,[43] polystyrene colloidal particles,[44] nickel foam,[45] alumina fiber blanket (AFB)[46] and even ice,[47] have been used. Note that these studies and development have been comprehensively reviewed.[27,48]

CVD methods, along with the solution template based method, are capable of fabricating these materials with highly defined structures. This might offer more ability to control the structures including the morphology of these materials required to optimize their catalytic activity.

WET CHEMISTRY APPROACHES FOR 3DGRAPHENE MATERIALS

Another main approach to synthesize 3D cross-linked graphene materials is to use the wet chemistry method with graphene oxide as the starting material. The rich functional groups, such as OH, COOH, C=O, and even C-H at the edge on the graphene sheets, can be used to cross-link directly them together using rich organic chemistry via ester, ether or even C-C bond. Also, with rich organic chemistry, many bifunctional organic/polymeric molecules can also be used to bridge these graphene sheets together. Since such 3DGraphene materials cross-linked by other molecules have been summarized in many works[5,49], and these materials in general exhibit a combination of graphene and other components, this type of materials will not be covered in general in this perspective.

For the preparation of additive-free cross-linked 3DGraphene, the earliest report should come from Shi's group, who in 2010 reported a highly electrically conducting and mechanically strong self-assembled graphene hydrogel (SGH) consisting of cross-linked graphene sheets using a hydrothermal process (Figure 4A).[50] Initially, the holding force between the sheets for the increased stability and mechanical strength was proposed to be the π-π stacking interaction between the graphene sheets. However it is believed that co-valent cross-bonding between the sheets at the edge should be generated in such hydrothermal treatment.[16] With such a highly interconnected 3D network structure, the hydrogel exhibits both remarkable electrical conductivity and mechanical robustness and thus renders it an excellent material for flexible energy storage device and other applications.[51] Additionally, the porous

microstructures and mechanical properties of the generated graphene sponges could be adjusted and controlled somehow by changing the parameters of the process.[52]

Later on, this method has been used widely and further developed. For example, when proper size of the graphene (oxide) units is used and processed in organic solvents, such as ethanol or acetone, the cross-linking between the sheets can be controlled better. Thus, a solvothermal method has been developed, and using such a method, a unique and highly elastic graphene-only 3D cross-linked graphene has been obtained (Figure 4B).[12,16] Intensive and various structural and morphology analyses prove that a monolithic 3D chemically linked network of graphene sheets is indeed formed in such spongy material. The cross-linking is mainly due to the covalent cross-linking of the functional groups such as OH, COOH and epoxy groups mainly located on the GO sheets edges, which generates such a monolithic 3D chemically linked graphene network. This monolithic and cross-linked graphene homogenous material, additive-free with only graphene units, indeed exhibits many interesting and unique properties at macroscale, including zero Poisson's ratios and super elasticity in all directions and under large strain,[16] and excellent organic liquid absorbing capability.[53]

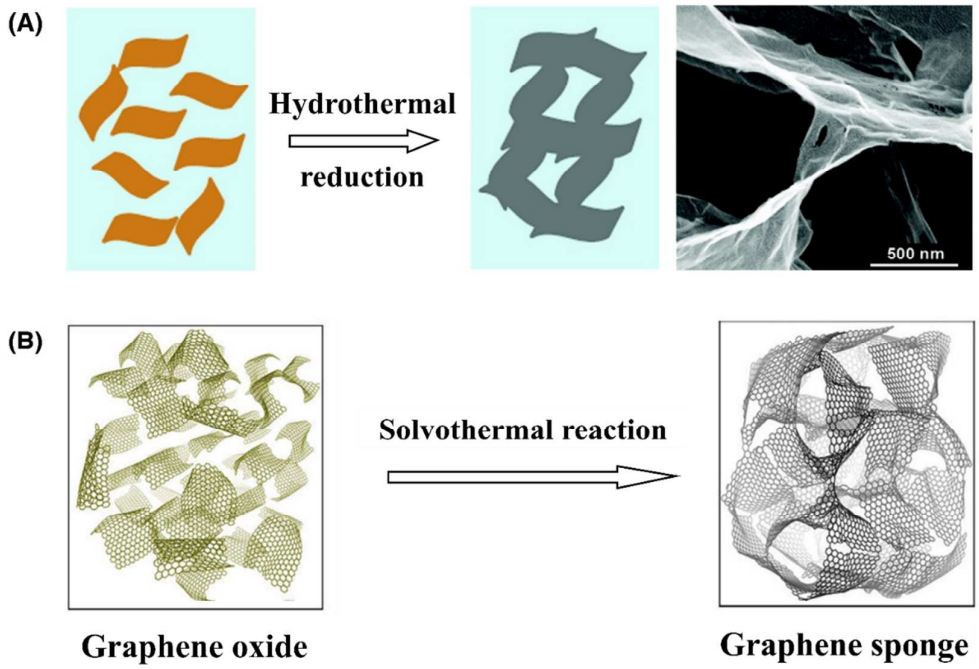

Figure 4. (A) The proposed formation mechanism for 3DGraphene. (Right) A typical SEM image of its interior microstructures. Reproduced with permission from ref 50. Copyright 2010, American Chemical Sociey. (B) The synthesis and structure of graphene sponges. Reproduced with permission from ref 16. Copyright 2015, Nature Publishing Group.

Linking the 2D graphene sheets using other molecules is another strategy to build the 3DGraphene network. One example came from Sudeep *et al*. group, where an ordered and stacked macroscopic 3D cross-linked nanoporous architecture via covalently interconnecting graphene sheets using organic molecule GAD has been reported (Figure 5).[54] The prepared 3D architectures with high hierarchical ordered morphology of uniform porosity and 3D conductive graphene scaffolds have

demonstrated potential applications such as for gas storage and electrochemical electrodes.

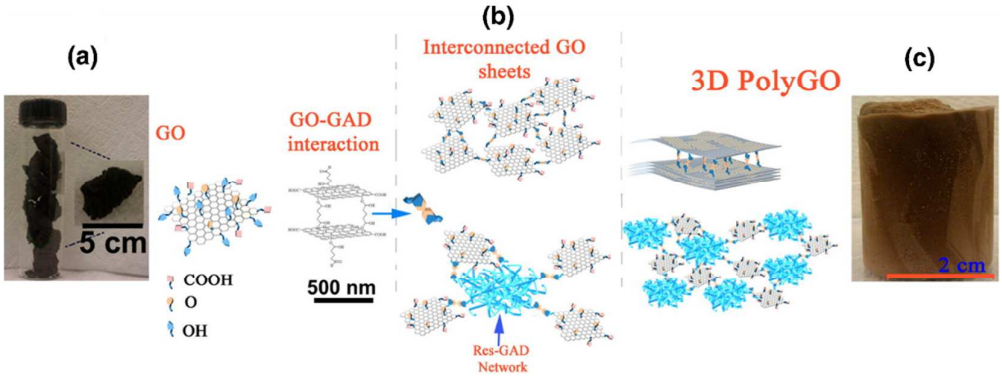

Figure 5. Schematic of the poly-GO synthesis process from initial GO powder. (a) Photograph showing the synthesized GO powders (left). (b) The linkage of glutaraldehyde (GAD, yellow) with two different –OH groups (blue); Two different mechanisms for large-scale GO cross-linking via pure glutaraldehyde (top) and via glutaraldehyde- resorcinol (bottom). (c) The 3D networked structure of poly-GO formed via two different mechanisms. Reproduced with permission from ref 54. Copyright 2013, American Chemical Society.

Another interesting wet chemical approach but using a 3D template was demonstrated by Chen *et al*.,[55] who constructed 3DGraphene porous material (ERGO) in-situ on the surface of an electrode by electrochemically reducing a concentrated graphene oxide dispersion based on the principle of graphene 3D self-assembly. Moreover, the electrochemical reduction of GO can be carried out on different types

of electrode, including graphene paper, foamed nickel and platinum foil. The electrochemical reduction of GO on the graphene paper leads to the formation of a flexible graphene-based electrode in which ERGO layer tightly adheres to the substrate of graphene paper, a promising electrode for many electrochemical applications.

REDOX CATALYTIC APPLICATIONS OF 3DGRAPHENE MATERIALS

One of the most important types of catalytic reactions are the redox reactions, which all involve electron transfer. Due to the rich and large π conjugation in graphene sheets and the similarity of its building unit (benzene ring) with aromatic or conjugated compounds, it is intuitive to believe that graphene materials must have strong interactions with such substrates and can prompt electron transfer for catalytic redox reactions. With the structural stability of 3DGraphene, the large 3D network would offer extra benefits for catalytic activity due to the excellent charge mobility for electron transfer. Furthermore, heteroatoms such as N, P, B, S etc. could be incorporated into graphene sheets, offering more possible active sites.[56] Together with the advantages as a 3D template to host other active materials for co-catalysts, 3DGraphene materials would therefore be promising materials for many catalytic redox reactions.

In this content, we will focus on the recent development and perspective of these materials as metal-free catalysts for the currently most studied catalytic reactions, ORR and HER, which play a vital role in the development of renewable energy sources. Since the major 3DGraphene materials used for these catalytic reactions come with some types of doped atoms, the following section will cover these doped materials first. Also, due to the extreme importance of CO_2 reduction which also belongs to redox reaction, though it has been not widely studied, it will be covered briefly in the last part of this section.

1. Oxygen Reducing Reaction

The oxygen reducing reaction, a crucial reaction occuring on the cathode to enable the fuel cell to work efficiently, plays an important role in the energy conversion devices of fuel cells and metal-air batteries.[57-59] Along with the rapid development of carbon nanomaterials, various carbon based and metal-free electrocatalysts have been exploited, exhibiting electrocatalytic activities comparable or even better than that of the noble metal catalysts and with better stability and fuel tolerance.[60] Some recent ORR studies using 3DGraphene based materials have been summarized and compared in Table 1.

Among these recently studied metal-free catalysts, materials with 3D cross-linked networks from doped graphene sheets have been widely studied as metal-free electrocatalyst for ORR due to the synergic effect combing the intrinsic nature of graphene, the unique structure and characteristics of 3DGraphene, and the

extra effect from doped atoms. These include catalysts with one-type heteroatom or multi-types of doped atoms, including nitrogen, phosphorus, boron, and sulfur atoms.

In 2011, Huang's group prepared a 3D nitrogen doped carbon nanotubes/graphene (NCNTs/G) composite by pyrolysis of pyridine over a graphene sheet supported Ni catalyst.[61] Tangled NCNTs with lengths of several hundred nanometers are sparsely, but tightly distributed on graphene sheets, forming quasi-aligned NCNT arrays. With 6.6 at. % N content, the NCNTs/G shows a higher activity and selectivity to ORR in alkaline electrolyte. In 2012, Qu's group fabricated an ultralight and nitrogen doped 3D cross-linked graphene framework (GF) through a hydrothermal reaction of GO aqueous suspension and pyrrole followed by a high temperature annealing process, and this material consists of mainly the network of only few graphene layers, and has an ultra-low density of 2.1 ± 0.3 mg/cm^3.[62] Besides the remarkable adsorption capacity and excellent capacitor performance, the macroscopic monolithic material with a tunable hierarchical morphology and high specific surface area shows extremely high activities for electrocatalytic ORR. A slightly lower onset potential of ORR on GF (*ca.* - 0.18 V) and notably higher diffusion current density over a large potential range (-0.4 to - 0.8 V) than that of Pt/C electrodes, as well as excellent tolerance of the GF electrode to the crossover effect were observed. The excellent performance is attributed to the unique 3D pore rich structure with maximum access to the nitrogen sites within highly exposed graphene sheets and multidimensional electron transport pathways. In 2015, nitrogen doped 3D

macroporous graphene (N-MGPPy) and porous graphene foams (PNGFs) were prepared by electrochemically and hard templating approaches, respectively.[63,64] Both of them exhibit excellent catalytic activities for ORR owing to the 3D porous structures and the nitrogen active sites of the electrode materials.

Compared with single-atom doped cases, the bi-atom or co-doped catalysts can deliver better catalytic activity due to the synergetic effect of different dopants. One excellent work came from the Dai group's systematic investigation for a three-dimensional nitrogen and phosphorus co-doped mesoporous carbon foams (NPMC) used for Zn-air battery. The material was fabricated using a scalable, one-step process involving the pyrolysis of a polyaniline aerogel synthesized in the presence of phytic acid (Figure 6a-d), and exhibits outstanding catalytic activities for both oxygen reduction and oxygen evolution reactions.[65] The electrochemical performance of the N,P-doped carbon foam as an air electrode for both primary and rechargeable Zn–air batteries was also investigated. Typically, an open-circuit potential of 1.48 V, a specific capacity of 735 mAh/g_{Zn} (corresponding to an energy density of 835 Wh/kg_{Zn}), a peak power density of 55 mW/cm^2, and stable operation for 240 h with mechanical recharging in primary batteries were obtained in an aqueous KOH electrolyte. A three-electrode rechargeable battery built with two NPMC metal-free air electrodes to have ORR and OER separately also demonstrated good stability (600 cycles for 100 h of operation). The carbon foam electrode material for both OER and ORR in a three-electrode configuration shows remarkable activity

with a positive onset potential of 0.94 V versus reversible hydrogen electrode (RHE) and a half-wave potential of 0.85 V versus RHE, which are comparable to those of Pt/C (Figure 6e-f). Density functional theory (DFT) calculations, together with experimental results, indicate that the excellent catalytic activity came from the synergistic effect of the N,P co-doping and highly porous graphene network and the main active sites are located at the doped edge positions of graphene network. Later on, they prepared another N,P-co-doped 3D porous carbon network (MPSA/GO) used as the catalysts for ORR/HER through a template free approach by pyrolysis of a supermolecular aggregate of self-assembled melamine, phytic acid, and graphene oxide. Zn-air batteries based on this MPSA/GO air electrode also show a high peak power density (310 W/g) and excellent durability.[58]

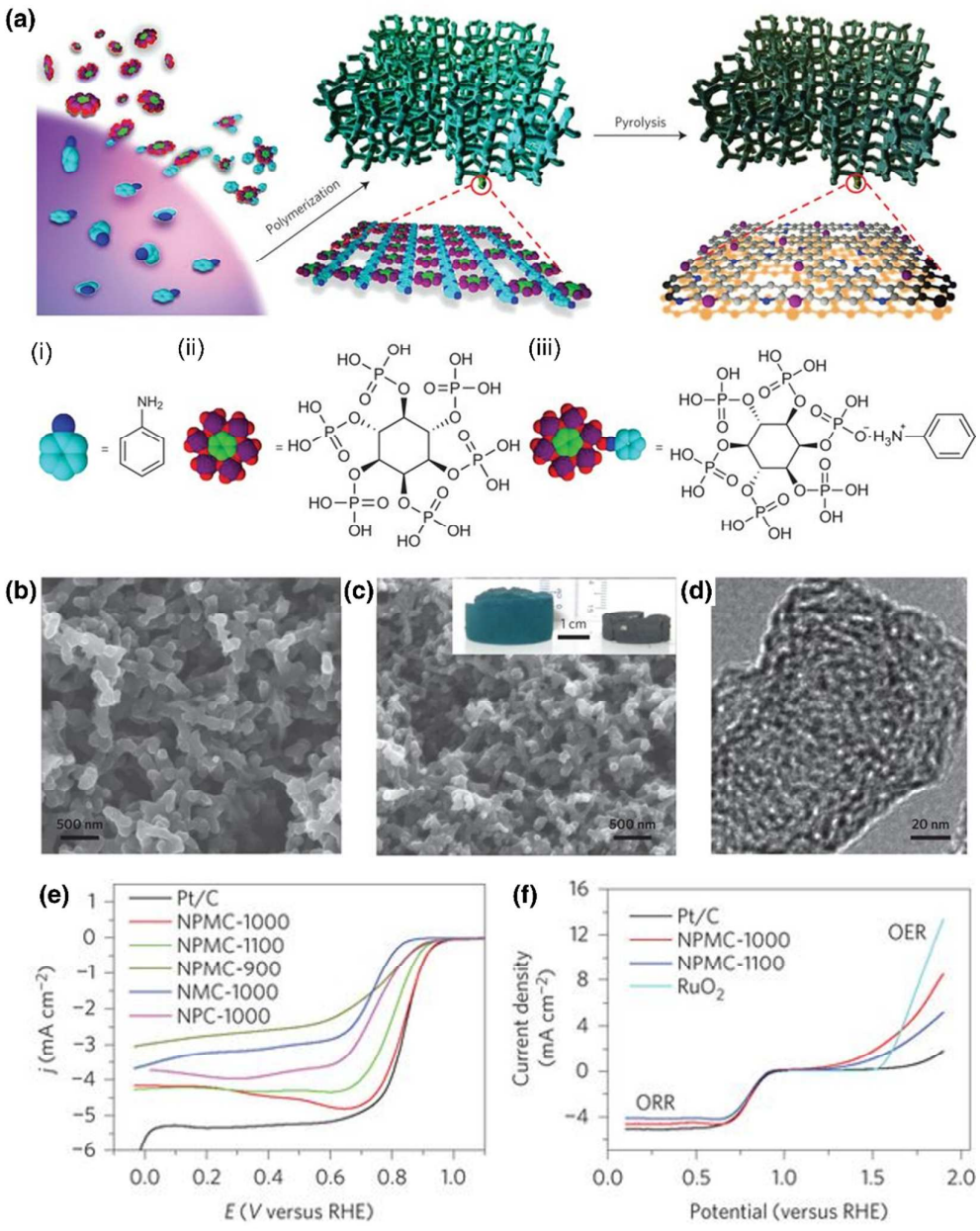

Figure 6. Preparation of N and P co-doped porous carbon (NPMC) electrocatalysts of (a) Schematic illustration of the preparation process for NPMC foams. (b,c) SEM images of PANi aerogel (b) and NPMC-1000 (c). Inset in c: Digital photo images of PANi aerogel before (left) and after (right) pyrolysis at 1,000 °C. (d) High-resolution TEM image of NPMC-1000. Electrocatalytic activity for ORR and OER of (e) Linear

scan voltammogram (LSV) curves for NPMC samples prepared under different temperatures and commercial Pt/C catalyst at an RDE (1,600 r.p.m.) in O_2-saturated 0.1M KOH solution. Scan rate, 5 mV/s, and (f) LSV curves of NPMC-1000, NPMC-1100, RuO_2 and commercial Pt/C catalyst on an RDE (1,600 r.p.m.) in 0.1M KOH (scan rate, 5 mV/s). Reproduced with permission from ref 65. Copyright 2015, Nature Publishing Group.

Besides N,P-co-doped materials, N,B co-doped 3DGraphene has also attracted a lot of attention. In 2013, a 3DGraphene foam co-doped with nitrogen (4.5 atom %) and boron (3 atom %) (BN-GFs) was prepared by a CVD method using melamine diborate as the precursor,[38] and it shows significantly better electrocatalytic activity towards ORR than the undoped and B or N mono-heteroatom doped foams, even slightly better than the compared Pt - C/GC electrode in 0.1 M KOH aqueous solution, including higher reduction peak current, more positive onset potential and higher stability. The reaction kinetics studies indicate that the number of electrons transferred per oxygen molecule is 3.4 - 3.8 at the potential range from -0.2 to -0.5 V. The excellent catalytic activities were contributed to the following reasons: 1) both the isolated N and B atom sites can act as active sites for ORR through charge transfer with neighboring C atoms; 2) interaction between adjacent N and B atoms could reduce the bandgap energy to further facilitate the ORR performance of the BN-GF electrode; 3) B and N co-doping could also enhance the electroactive surface area

significantly. Then in 2015, Xu *et al*. also demonstrated similar results, where based on the synergistic coupling of the B and N dopants within the graphene domains, the dual 3D N/B-doped graphene aerogel (foam) (N,B-GA) prepared by a hydrothermal reaction and a pyrolysis procedure showed superior catalytic activity for the ORR than that of the single N or B doped materials.[66] Nitrogen and sulfur could also act together as the co-doped heteroatoms to 3DGraphene for catalytic purpose materials. In 2013, Feng's group reported nitrogen/sulfur co-doped 3DGraphene frameworks (N/S-GFs) prepared by a one-pot hydrothermal approach employing graphene oxide and ammonium thiocyanate as the precursors, and achieved an excellent catalytic behavior for ORR in alkaline condition.[67] Later, similar works have been reported also by several other groups.[68-70]

Besides doped 3DGraphene materials, some 3DGraphene prepared by cross-linking with organic small molecules have been also investigated for catalytic purposes. For example, Kim's group reported a novel 3DGraphene material prepared through covalent amidation reaction using diamine compounds and has studied them as a metal-free electrocatalyst for ORR in alkaline media.[71] It has been proposed that the linking compounds used as a junction between functionalized rGO layers improve the electrical conductivity and impart electrocatalytic activity for ORR due to the facilitated interlayer charge transfer. Investigation of the ORR mechanism reveals that higher pyridinic-like N content and π-electron interaction-free interlayer charge transfer contributed to their higher catalytic activities and stability than that of the

compared materials prepared from nonfunctionalized rGO. Similarly, using glutaraldehyde as the cross-linking agent, a 3D cross-linked graphene based electrocatalytic catalyst with high activity was assembled by individual 2D graphene nanoribbons.[72] With ultrathin g□C_3N_4 nanosheets and hexagonal boron nitride as additional agents respectively, 3DGraphene based composites have been synthesized and delivered outstanding catalytic activities for ORR owing to the synergistic effects of the graphene network and the additional agents resulting into active centres.[73,74]

In the works discussed above, where doped 3DGraphene or 3DGraphene hybrids with other additional components have been studied for their catalytic activity, the active sites of these catalysts come mainly from the foreign atoms (sites) doped on the intrinsic atoms (sites) of graphene. As has been noted and discussed above, when other agents are introduced to graphene, its intrinsic properties will be largely impaired and cannot be fully utilized. So, it would be highly interesting to study the catalytic activity of pristine 3DGraphene without any doped or hybrid agents.

Based on this, Zhang et al. have studied thermally treated 3DGraphene prepared directly by heating GO without any other foreign atoms or doped agents as a highly efficient metal-free electrocatalyst towards ORR.[75] Interestingly, they pointed out that the breaking up of the initial C=O bonds in the 3DGraphene materials during the high temperature treatment (600 °C) would leave vacant sites at the original C=O positions. The synergetic effect between broken C=O bonds on 3DGraphene and its unique porous structure generated competitive catalytic activity, higher selectivity and better

stability toward ORR compared with that of commercial Pt/C. While it has not been fully studied, it is believed that the observed catalytic activity should come mainly from the defect (vacant) sites generated by the decomposition of some functional groups including C=O as the authors indicated. Also, the unique porous structure of 3DGraphene materials are able to trap oxygen molecules more efficiently, contributing to a decrease in the diffusion resistance and enhancing electrolyte-electrode accessibility for fast mass transport. Note that the catalytic studies for pristine 3DGraphene are very limited so far and the measured catalytic activity is still lower than some doped 3DGraphene.[38,64] Thus, many more studies for this type of graphene material are needed to fully capitalize their catalytic potential, including controlling and optimizing defect and vacant sites, which is believed to be the main source of the catalytic activity.

Table 1. Summary and comparison of some recent reported typical 3DGraphene based materials for ORR in terms of their structural characteristic, catalytic performance and the activity origin.

3DGraphene based material	**Structural characteristics**	**Catalytic performance**	**Proposed main (high) activity origin**	**Ref.**
3D NCNTs/G	N doping	$E_{onset} \sim -0.191$ V *vs.* SCE in alkaline electrolyte, slightly lower than that of the Pt/C; diffusion current close to that of the Pt/C	Nitrogen doping	61
3D GF	N doping	$E_{onset} \sim -0.18$ V *vs.* SCE in alkaline electrolyte, slightly lower than that of the Pt/C; higher	3D pore rich structure with maximum access to the N sites	62

		diffusion current density than that of Pt/C over a large potential range from – 0.4 to – 0.8 V	within highly exposed graphene sheets and multidimensional electron transport pathways	
PNGFs	N doping	ORR activity and long term stability in both alkaline and acidic solutions; E_{onset} of 1.02 V *vs.* RHE in alkaline solution (diffusion current density of *ca.* 7 mA/cm^2) and 0.83 V in acidic media	N doping, large specific surface area and diversified porosity	63
3D nN-MGPPy	N doping	E_{onset} of – 0.132 V *vs.* Ag/AgCl in alkaline electrolyte; a current density value of 5.56 mA/cm^2	High SSA and conductivity of graphene network; high mass transport rate owing to the 3D porous structure;	64
3D NPMC	N and P co-doping	High activities toward both ORR and OER in alkaline electrolyte. For ORR, E_{onset} of 0.94 V *vs.* RHE and a half-wave potential of 0.85 V in alkaline solution; For Zn–air battery based on NPMC, an open-circuit potential of 1.48 V, a specific capacity of 735 mAh/g$_{Zn}$ (corresponding to an energy density of 835 Wh/kg$_{Zn}$), a peak power density of 55 mW/cm^2, and stable operation for 240 h	Synergistic effects of N, P co-doping and graphene edge effects for the catalytic activities towards both OER and ORR	65
3D MPSA/GO	N and P co-doping	High activities toward both HER and ORR. For ORR, a comparable E_{onset} and kinetic current density to that of Pt/C. For Zn–air battery, a high peak power density of 310 W/g and an excellent durability without potential drop over 90 h.	Synergistic effects of N,P co-doping; 3D porous graphitic network for the electron and electrolyte transports and the stabilities	58
3D GF	N and B co-doping	E_{onset} of *ca.* – 0.16 V *vs.* SCE in alkaline electrolyte; a current density of 7.8 mA/cm^2 at – 0.03 V; excellent stability with 89% current retention after 20000 s.	Doped N and B atoms act as active sites; interaction between adjacent N and B atoms reduces the bandgap energy; also the increased electroactive surface area	38
3D GF	N and B co-doping	E_{onset} of – 0.07 V *vs.* SCE in alkaline electrolyte; a higher diffusion current density.	Large SSA, 3D interconnected framework; macro/mesoporosity structures ensuring accessible porosity and effective mass transport; high nitrogen and boron content, dominant active pyridinic	66

			and graphitic nitrogen and BC3 species; synergistic effect of N and B	
3D N/S-GFs	N and S co-doping	A current density of 3.90 mA/cm^2 in alkaline electrolyte; excellent stability with current density retention of 85.2 % over 20,000 s	N and S co-doping	67
3D GF	N and S co-doping	A current density of about 0.17 mA/cm^2 at a voltage of 0.7 V in alkaline electrolyte	Edge effect and heteroatom synergistic effect	68
NS-3DrGO	N and S co-doping	E_{onset} of 0.895 V *vs.* RHE in alkaline electrolyte; diffusion-limiting current of 5.23 mA/cm^2 at 0.2 V.	High amount (74.8 at. %) of pyridinic N and graphitic N; high amount (79.8 at. %) of active thiophene-S; high specific surface (391.9 m^2/g) area and multi-porous structure	69
3D NSGAs	N and S co-doping	E_{onset} of – 0.1 V *vs.* Ag/AgCl in alkaline electrolyte; kinetic current density of 26.1 mA/cm^2	Synergistic coupling of N and S resulting in more exposed "active sites" in graphene frame	70
3D GF	cross-linking via covalent amide	E_{onset} of − 0.1 V *vs.* Ag/AgCl in alkaline electrolyte; higher limiting diffusion current density than that of Pt/C electrode at large potential range	Increased SSA, hierarchical porous structure, and sp^3-amide linkage between rGO layers	71
3D GNRs	cross-linking via glutaraldehyde	An increased peak current compared with the GNR modified electrodes; a slight change in the onset potential	Well interconnected and porous; high SSA and fast electron transfer	72
3D g-C_3N_4/rGO	cross-linking of g-C_3N_4 and GO	E_{onset} of – 0.21 V *vs.* Ag/AgCl in alkaline electrolyte; a wave current enhanced by 1.6 and 2.3 times compared with g-C_3N_4 and rGO; superior durability over Pt/C catalyst	g-C_3N_4 nanosheets as active centers; rGO sheets as "highways" for electron transport; an efficient 3D electron transport network	73
3D rGO/BN	wrapping of BN sheets into graphene network	E_{onset} of 0.798 V *vs.* RHE in alkaline conditions; a current density of 3 mA/cm^2; higher stability than commercial Pt/C catalysts even after 10000 cycles	Synergistic effect of the carbon network and B–N, resulting into active centers for ORR kinetics	74
3DG	without any other foreign atoms or doped agents	E_{onset} close to that of Pt/C electrode; higher stability than that of Pt/C electrode.	Synergistic effect between broken C=O bonds and the unique porous structure of 3DGraphene	75

2. Hydrogen Evolution Reaction

The hydrogen evolution reaction is a vital catalytic reaction that could be conducted by either photo- or electro-catalysis, and both approaches have been intensively studied in the past few decades using various carbonaceous (metal-free) materials, including recently with 3D cross-linked bulk graphene based material and the semiconductor but graphene-like polymeric 3D cross-linked g-C_3N_4. The efficient light absorption, tunable and no-zero but tunable band gap and its 3D conjugation network makes these materials particularly attractive for photocatalytic HER. Thus, in this section photocatalytic HER will be covered first, followed by electrochemical HER using these materials.

2.1 Photocatalysis

The intrinsic zero bandgap of pristine graphene has been limiting its direct application as a photocatalyst. Thus, the most commonly reported graphene based photocatalysts come from either heteroatom (e.g. N, S, B, P) doped graphene, chemically modified graphene materials (e.g. GO and reduced GO) or hybrid/composites where graphene is used as an electron acceptor or conductor and is combined with other semiconductors.[76] Among the metal-free 3D cross-linked carbon based catalysts, the graphene-like polymeric material g-C_3N_4 is probably the most studied. Thus, we will cover this material first.

Early in 2009, Wang and colleagues reported the catalytic hydrogen production activity from water under visible-light irradiation using old polymeric carbon nitrides (g-C_3N_4) for the first time as a metal-free photocatalyst.[77] With their impressive optical properties, electronic structures as well as a 2.7 eV bandgap, the polymeric material exhibits an intrinsic semiconductor-like absorption with energetically possibility for water splitting (Figure 7A). The g-C_3N_4 achieved steady H_2 production with a rate of 0.1-0.4 μmol/h from water and triethanolamine as a sacrificial electron donor on light illumination (> 420 nm) in the absence of noble metal catalysts. Comparing the activity results of different materials prepared under different temperatures, they pointed out that some defect structures are crucial, which might facilitate the charge localization at specific surface termination sites where they can be transferred to the water molecules.

Although intensive studies of polymeric g-C_3N_4 as a metal-free catalyst for water splitting have been reported following this pioneering work,[78,79] the reactions still suffer from a low hydrogen production and quantum efficiency (QE) and also require a sacrificial reagent.[80] Until 2015, Lee's group constructed carbon a dots/g-C_3N_4 composite (CDots-C_3N_4) photocatalyst for water splitting under visible light.[81] The low-cost and environmentally benign materials can achieve QEs of 16% to split water into H_2 and O_2 at a wavelength of 420 nm, and also demonstrated a robust stability in 200 runs of recycling use over 200 days. A 2.0% of overall solar energy conversion efficiency, at least one order of magnitude larger than previous reports for any stable

water splitting photocatalyst, was achieved (Figure 7B). Different from the one-step four-electron mechanism of conventional photocatalysis, the impressive performance of this composite catalyst is believed to have a stepwise two-electron/two-electron two-step pathway, where H_2O oxidation to H_2O_2 is the first and rate limiting step (photocatalysis), and for the second and fast step (chemical catalysis) CDots are responsible for decomposing H_2O_2 to O_2 and finishing the entire catalytic cycle.

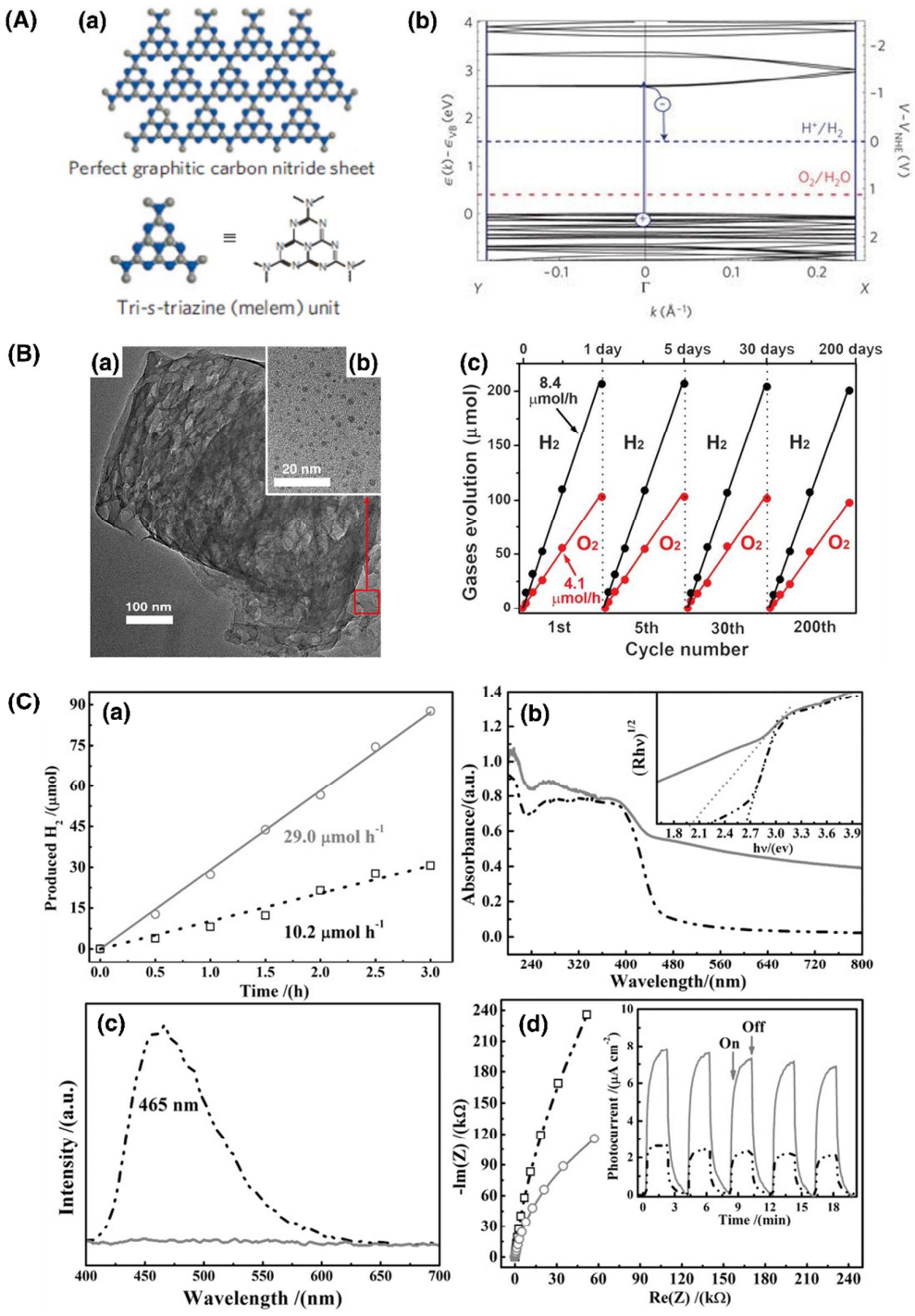

Figure 7. (A) Crystal and electronic structure of graphitic carbon nitride (g-C_3N_4) (a) Schematic diagram of a perfect graphitic carbon nitride sheet constructed from melem units. (b) DFT band structure for polymeric melon calculated along the chain (*Γ*–*X*

direction) and perpendicular to the chain (*Y–Γ* direction). Reproduced with permission from ref 77. Copyright 2009, Nature Publishing Group. (B) Characterization of the physical structure and photocatalytic water-splitting performance of the CDots-C_3N_4 composite catalyst. (a) A TEM image and (b) magnified TEM image of the CDots-C_3N_4 region of (a) marked in red. (c) Typical time course of H_2 and O_2 production from water under visible light irradiation. Reproduced with permission from ref 81. Copyright 2015, American Association for the Advancement of Science. (C) The performance of catalyst. (a) Photocatalytic activity for H_2 production, (b) DRS spectrum, (c) PL emission spectra, and (d) EIS plot and photocurrent-time dependence of PCNM (solid line) and the g-CN powder (dotted line). Reproduced with permission from ref 82. Copyright 2015, Wiley-VCH.

Following the exciting development of the C_3N_4 catalyst above, a macroscopic 3D porous g-C_3N_4 monolith (PCNM) consisted of 2D porous C_3N_4 nano-sheets was synthesized by Yang's group through one-step thermal polymerization of urea inside the framework of melamine sponge (MS).[82] With a large specific surface area (SSA), multiple junctions and open pores, the unique 3D interconnected network of PCNM exhibits significantly improved photocatalytic performance for hydrogen evolution under visible light compared to the powder counterpart catalyst (Figure 7C-a). The significantly enhanced catalytic activity compared to that of the powder g-C_3N_4 is believed due to the following reasons: 1) larger SSA; 2) more efficient light

absorption light (Figure 7C-b); 3) better separation of photo-generated charge carriers (Figure 7C-c) and faster interface charge transport (Figure 7C-d).

While it is rare, additive/doping free 3DGraphene has also been studied for its photocatalytic HER. We have exploited such a monolithic homogenous and cross-linked 3DGraphene material for photocatalytic HER which followed a very unique mechanism.[83] The combination of its unique band structure of graphene and macroscopic morphology of this material ensures an efficient light absorption of graphene and an easily achievable reverse saturation state under light illumination.[12] All these together makes it capable of ejecting efficiently hot electrons under visible illumination and thus capable for wide redox chemical conversion. Thus for the first time, a carbon-only 3DGraphene catalyst for efficient water splitting to generate H_2 has been achieved under visible light. This material exhibits a remarkable hydrogen production rate of 270 μmol/h/g_{cat} under full-spectrum light (Figure 8) following a light-induced ejected hot-electron relaxing mechanism.[83]

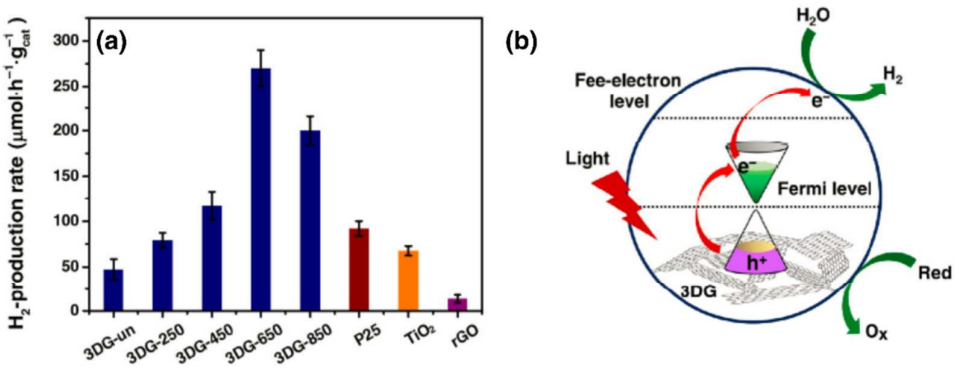

Figure 8. Photocatalytic hydrogen evolution activities from water splitting. (a) Production rate over a series of 3DG samples synthesized at various annealing. (b) Pathways of electron transfer and mechanism of photocatalytic hydrogen production catalyzed by 3DG. Reproduced with permission from ref 83. Copyright 2017, Springer Nature.

2.2 Electrocatalysis

For electrocatalysis HER, the highly conductive cross-linked network existing in 3DGraphene is expected to facilitate exciton charge separation and also charge transportation during the process of HER. Furthermore, the rich macropores in these 3D structures should provide a facilitated electrolyte accessing to the inner structure of the catalysts and improve overall the HER kinetics.[27]

By rationally engineering the macroscopic architecture of graphene and its chemical/defective structures, Tian *et al*. designed a 3D N-doped and plasma-etched graphene (3DNG-P) and used it as a HER catalyst.[84] Combined the merits of

freestanding 3D porous architecture, high-level N-doping and plasma-induced enriched defects, the prepared 3DNG-P leads to an excellent electrocatalytic performance for HER with both highly enhanced activity with a low overpotential of 128 mV at 10 mA/cm^2 and stability over a wide pH range. The authors proposed that the enhanced catalytic performance is attributed to the following reasons: 1) the 3D architecture affords efficient electron/ion-transport pathways to lower the HER polarization resistance; 2) both N dopants and plasma-induced defects offer more active centers for HER; and 3) the coupling of N dopants with graphene defects produces a synergistic effect in further enhancing the HER activity of the active centers.

Combing doped graphene and carbon nitride, a metal-free electrocatalyst (CN_x@N-RGO) has been prepared by annealing GO-soaked melamine foam, which produced a three dimensional nanostructure consisting of nitrogen doped graphene (N-RGO) layers distributed on the interconnected arms of carbon nitride (CN_x) tetrapods (Figure 9).[85] As an electrocatalyst for HER, it shows rather low overpotential of 193 mV to reach a high current density of 10 mA/cm^2 and low Tafel slope value of 54 mV/dec, following a Volmer-Heyrovsky mechanism. The study shows that the structural modifications and spatial rearrangement of N-RGO on CN_x provides a high density of in-plane nitrogen coordinated active centers, whereas the 3D macroporous morphology assists efficient reactant/product distribution. Furthermore, DFT calculations show that the synergy between CN_x and N-RGO

facilitates good electrical coupling between the two moieties and provides optimal binding to H^+ ions on the catalyst, which in turn results in efficient reduction of hydrogen ions.

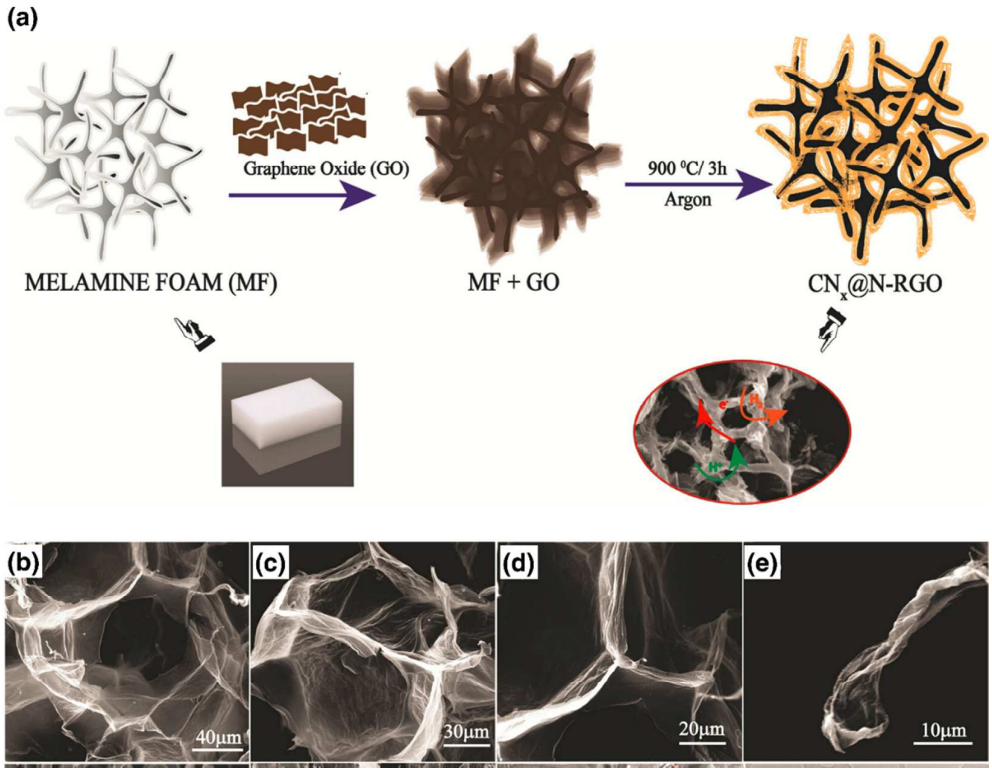

Figure 9. (a) A pictorial representation illustrating the preparation of the CN_x@N-RGO catalyst using melamine foam and GO. (b,c) SEM images representing an interconnected 3D network of CN_x@N-RGO at different magnifications. (d) The tetrapod structure of CN_x@NRGO; e) the single arm of the tetrapod of CN_x@N-RGO, showing the wrapping of the arm by the N-RGO sheet. Reproduced with permission from ref 85. Copyright 2017, Wiley-VCH.

3. CO_2 Reduction

As a visible-light responsive photocatalyst for CO_2 reduction, Tong *et al*. designed a 3D porous g-C_3N_4/graphene oxide aerogel (CNGA) by a hydrothermal co-assembly of 2D g-C_3N_4 and GO nanosheets, in which g-C_3N_4 acts as an efficient photocatalyst, and GO supports the 3D framework and also promotes the electron transfer simultaneously.[86] Excellent photocatalytic performance with a high yield of CO of 23 mmol/g (within 6 h) from CO_2 reduction was achieved. The mechanism studies indicate that the enhanced photocatalytic activity of CNGA is due to the synergetic effect of both graphene and C_3N_4 moieties: 1) the photogenerated electrons from g-C_3N_4 can be transferred to graphene network due to their large coherent interface, thus the radiative recombination of electron−hole pairs was significantly inhibited; 2) the 3D porous aerogel structure of CNGA is beneficial to the visible-light absorption and promoting more electron−hole pairs; 3) the high adsorption capacity and rapid mass transport due to the 3D porous framework are kinetically favorable for the surface chemical reaction.

In 2015, Ajayan group prepared a N-doped 3DGraphene foam through ambient-pressure CVD method followed by post-doping with a solid nitrogen rich precursor graphitic-C_3N_4 and studied this material for CO_2 reduction.[42] The 3DGraphene foam incorporated with nitrogen defects as a metal-free catalyst for CO_2 reduction shows a negligible onset overpotential (−0.19 V) for CO2 reduction to CO

formation, and exhibits superior activity over Au and Ag, achieving similar maximum Faradaic efficiency for CO production (~85%) at a lower overpotential (−0.47 V) and better stability for at least 5 h. Furthermore, both theoretical calculations and experimental results suggest pyridinic-N is the most active site for CO_2 reduction. The structure and catalytic performance is shown in Figure 10.

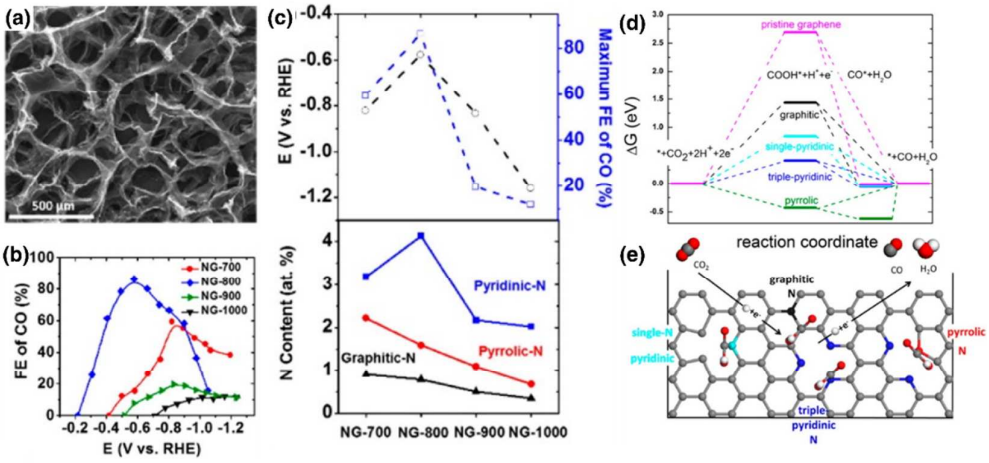

Figure 10. The morphology of (a) A SEM image showing a representative graphene foam with an open frame structure. The electrocatalytic activities of N-doped graphene foam of (b) Faradaic efficiency of CO versus potential and (c) Maximum Faradaic efficiency of CO and its corresponding potential versus N functionality content. DFT modeling of electrocatalysis of CO_2 on NG of (d) Free energy diagram of electrochemical reduction of CO_2 to CO on NG and (e) schematic of N configuration and CO_2 reduction pathway. Reproduced with permission from ref 42. Copyright 2016, American Chemical Society.

CHALLENGE AND OUTLOOK

For the synthesis part, bulk and 3D cross-linked graphene materials and the likes such as g-C_3N_4 with monolithic 3D cross-linked networks of the 2D units, including the doped and hybrid ones are expected to offer a much better position to achieve the full potential of these 2D materials at the bulk state, and thus deserve much more attention and systematic studies. So far, all these prepared materials have neither uniform building units nor ordered structure. Thus, the truly challenging and extremely important task is to have some ordered 3D cross-linked structure with uniform graphene sheets as the building unit. These studies might also offer some exciting opportunities to win the war to fully realize the potential of graphene and bring the truly killer application of graphene on table.

Among all the proposed applications, owing to the combination of the excellent intrinsic properties of graphene and the 3D porous structures, 3D cross-linked graphene materials, including the doped and hybrid ones with g-C_3N_4, have demonstrated exciting catalytic potential compared to traditional metal based catalysts. The high or superior catalytic activity arise generally from the synergetic effect of the combination of several characteristics of these 3DGraphene or the like materials, including surface functional groups, doped heteroatoms and vacancies as the active sites, the collective properties of individual graphene sheet, strong adsorption and pre-absorption of reactants, the large 3D and porous cross-linked conjugation network

for efficient charge separation and transportation, high chemical and thermal stability, and etc. To achieve better/higher activity, the control of doping and vacant sites and their distribution and band structure is probably the first issue to address. Note since most of such materials so far do not have an ordered structure, and their exact structure is still unresolved, even the reproducibility of the preparation of these materials and their catalytic activity is another big issue. This again prompts the challenging task to have some ordered or crystalline 3D structure with graphene sheets as the building unit as mentioned above. Overcoming such a challenge will not only address many issues mentioned above for catalytic applications but should also have important implications for other graphene related applications. Though there have been many studies so far, the identification of the exact active location and nature of the catalytic active centers, and mechanism of catalysis are far from clear. All these issues require much more systematic studies before we can possibly utilize the important properties of 3DGraphene or the like materials for the extreme important catalytic application.

AUTHOR INFORMATION

Corresponding Authors

yschen99@nankai.edu.cn

yanhonglu@mail.nankai.edu.cn

Notes

The authors declare no competing financial interest.

ACKNOWLEDGEMENTS

The authors gratefully acknowledge the financial support from the Ministry of Science and Technology of China (MoST) (2016YFA0200200) and National Natural Science Foundation of China (NSFC) (51502125, 21421001, 51633002 and 51472124) of China, Tianjin city (16ZXCLGX00100), 111 Project (B12015), Foundation of Hebei Province of China (E2016408035, B2017408042) and the Research Project of Hebei Education Department of China (BJ2016044).

REFERENCES

(1) Geim, A. K.; Novoselov, K. S. *Nat. Mater.* **2007,** *6*, 183.

(2) Avouris, P.; Chen, Z.; Perebeinos, V. *Nat. Nanotech.* **2007,** *2*, 605.

(3) Meyer, J. C.; Geim, A. K.; Katsnelson, M. I.; Novoselov, K. S.; Booth, T. J.; Roth, S. *Nature* **2007,** *446*, 60.

(4) Li, D.; Kaner, R. B. *Science* **2008,** *320*, 1170.

(5) Ma, Y.; Chen, Y. *Natl. Sci. Rev.* **2015,** *2*, 40.

(6) Ramanathan, T.; Abdala, A. A.; Stankovich, S.; Dikin, D. A.; Herrera-Alonso, M.; Piner, R. D.; Adamson, D. H.; Schniepp, H. C.; Chen, X.; Ruoff, R. S.; Nguyen, S. T.; Aksay, I. A.; Prud'homme, R. K.; Brinson, L. C. *Nat. Nanotech.* **2008,** *3*, 327.

(7) Stankovich, S.; Dikin, D. A.; Dommett, G. H. B.; Kohlhaas, K. M.; Zimney, E. J.; Stach, E. A.; Piner, R. D.; Nguyen, S. T.; Ruoff, R. S. *Nature* **2006,** *442*, 282.

(8) Geim, A. K. *Science* **2009,** *324*, 1530.

(9) Du, X.; Skachko, I.; Barker, A.; Andrei, E. Y. *Nat. Nanotech.* **2008,** *3*, 491.

(10) Chen, W.; Xiao, P.; Chen, H.; Zhang, H.; Zhang, Q.; Chen, Y. *Adv. Mater.* **2018**, 10.1002/adma.201802403.

(11) Park, S.; Lee, K.-S.; Bozoklu, G.; Cai, W.; Nguyen, S. T.; Ruoff, R. S. *ACS Nano* **2008,** *2*, 572.

(12) Zhang, T.; Chang, H.; Wu, Y.; Xiao, P.; Yi, N.; Lu, Y.; Ma, Y.; Huang, Y.; Zhao, K.; Yan, X.-Q.; Liu, Z.-B.; Tian, J.-G.; Chen, Y. *Nat. Photon.* **2015,** *9*, 471.

(13) Kuc, A.; Seifert, G. *Phys. Rev. B* **2006,** *74*, 214104.

(14) Chang, H.; Qin, J.; Xiao, P.; Yang, Y.; Zhang, T.; Ma, Y.; Huang, Y.; Chen, Y. *Adv. Mater.* **2016**, 28, 3504.

(15) Lu, Y.; Long, G.; Zhang, L.; Zhang, T.; Zhang, M.; Zhang, F.; Yang, Y.; Ma, Y.; Chen, Y. *Sci. China Chem.* **2016**, 59, 225.

(16) Wu, Y.; Yi, N.; Huang, L.; Zhang, T.; Fang, S.; Chang, H.; Li, N.; Oh, J.; Lee, J. A.; Kozlov, M.; Chipara, A. C.; Terrones, H.; Xiao, P.; Long, G.; Huang, Y.; Zhang, F.; Zhang, L.; Lepro, X.; Haines, C.; Lima, M. D.; Lopez, N. P.; Rajukumar, L. P.;

Elias, A. L.; Feng, S.; Kim, S. J.; Narayanan, N. T.; Ajayan, P. M.; Terrones, M.; Aliev, A.; Chu, P.; Zhang, Z.; Baughman, R. H.; Chen, Y. *Nat. Commun.* **2015,** *6*, 7141.

(17) Zhang, Y.; Huang, Y.; Zhang, T.; Chang, H.; Xiao, P.; Chen, H.; Huang, Z.; Chen, Y. *Adv. Mater.* **2015,** *27*, 2049.

(18) Su, C.; Acik, M.; Takai, K.; Lu, J.; Hao, S.-J.; Zheng, Y.; Wu, P.; Bao, Q.; Enoki, T.; Chabal, Y. J.; Loh, K. P. *Nat. Commun.* **2012,** *3*, 1298.

(19) Deng, D.; Novoselov, K. S.; Fu, Q.; Zheng, N.; Tian, Z.; Bao, X. *Nat. Nanotech.* **2016,** *11*, 218.

(20) Voiry, D.; Shin, H. S.; Loh, K. P.; Chhowalla, M. *Nat. Rev. Chem.* **2018,** *2, 0150*.

(21) Zhao, Y.; Nakamura, R.; Kamiya, K.; Nakanishi, S.; Hashimoto, K. *Nat. Commun.* **2013,** *4*, 2390.

(22) Liu, X.; Dai, L. *Natl. Sci. Rev.* **2016,** *1, 16064*.

(23) Wu, J.; Ma, S.; Sun, J.; Gold, J. I.; Tiwary, C.; Kim, B.; Zhu, L.; Chopra, N.; Odeh, I. N.; Vajtai, R.; Yu, A. Z.; Luo, R.; Lou, J.; Ding, G.; Kenis, P. J. A.; Ajayan, P. M. *Nat. Commun.* **2016,** *7,* 13869.

(24) Yang, L.; Li, X.; Zhang, G.; Cui, P.; Wang, X.; Jiang, X.; Zhao, J.; Luo, Y.; Jiang, J. *Nat. Commun.* 2017, 8, 16049.

(25) Ji, X.; Zhang, X.; Zhang, X. *J. Nanomater.* **2015**, 357196.

(26) Nardecchia, S.; Carriazo, D.; Luisa Ferrer, M.; Gutierrez, M. C.; del Monte, F. *Chem. Soc. Rev.* **2013,** *42*, 794.

(27) Qiu, B.; Xing, M.; Zhang, J. *Chem. Soc. Rev.* **2018,** *47*, 2165.

(28) Wang, J.-T.; Nie, S.; Weng, H.; Kawazoe, Y.; Chen, C. *Phys. Rev. Lett.* **2018,** *120*, 026402.

(29) Mackay, A. L. *Nature* **1985,** *314*, 604.

(30) Terrones, A. L. M. a. H. *Nature* **1991,** *352*, 762.

(31) Zhao, Z. S.; Xu, B.; Wang, L. M.; Zhou, X. F.; He, J. L.; Liu, Z. Y.; Wang, H. T.; Tian, Y. J. *ACS Nano* **2011,** *5*, 7226.

(32) Lin, Y.; Zhao, Z.; Strobel, T. A.; Cohen, R. E. *Phys. Rev. B* **2017,** *94*, 245422.

(33) Ito, Y.; Tanabe, Y.; Qiu, H. J.; Sugawara, K.; Heguri, S.; Ngoc Han, T.; Khuong Kim, H.; Fujita, T.; Takahashi, T.; Tanigaki, K.; Chen, M. *Angew. Chem. Int. Ed.* **2014,** *53*, 4822.

(34) Chen, Z.; Ren, W.; Gao, L.; Liu, B.; Pei, S.; Cheng, H.-M. *Nat. Mater.* **2011,** *10*, 424.

(35) Nueangnoraj, K.; Nishihara, H.; Imai, K.; Itoi, H.; Ishii, T.; Kiguchi, M.; Sato, Y.; Terauchi, M.; Kyotani, T. *Carbon* **2013,** *62*, 455.

(36) Krainyukova, N. V.; Zubarev, E. N. *Phys. Rev. Lett.* **2016,** *116*, 055501.

(37) Pettes, M. T.; Ji, H.; Ruoff, R. S.; Shi, L. *Nano Lett.* **2012,** *12*, 2959.

(38) Xue, Y.; Yu, D.; Dai, L.; Wang, R.; Li, D.; Roy, A.; Lu, F.; Chen, H.; Liu, Y.; Qu, J. *Phys. Chem. Chem. Phys.* **2013,** *15*, 12220.

(39) Xiao, X.; Beechem, T. E.; Brumbach, M. T.; Lambert, T. N.; Davis, D. J.; Michael, J. R.; Washburn, C. M.; Wang, J.; Brozik, S. M.; Wheeler, D. R.; Burckel, D. B.; Polsky, R. *ACS Nano* **2012,** *6*, 3573.

(40) Yoon, J.-C.; Lee, J.-S.; Kim, S.-I.; Kim, K.-H.; Jang, J.-H. *Sci. Rep.* **2013,** *3*.

(41) Li, Y.; Li, Z.; Shen, P. K. *Adv. Mater.* **2013,** *25*, 2474.

(42) Wu, J.; Liu, M.; Sharma, P. P.; Yadav, R. M.; Ma, L.; Yang, Y.; Zou, X.; Zhou, X.-D.; Vajtai, R.; Yakobson, B. I.; Lou, J.; Ajayan, P. M. *Nano Lett.* **2016,** *16*, 466.

(43) Huang, X.; Qian, K.; Yang, J.; Zhang, J.; Li, L.; Yu, C.; Zhao, D. *Adv. Mater.* **2012,** *24*, 4419.

(44) Choi, B. G.; Yang, M.; Hong, W. H.; Choi, J. W.; Huh, Y. S. *ACS Nano* **2012,** *6*, 4020.

(45) Ji, J.; Liu, J.; Lai, L.; Zhao, X.; Zhen, Y.; Lin, J.; Zhu, Y.; Ji, H.; Zhang, L. L.; Ruoff, R. S. *ACS Nano* **2015,** *9*, 8609.

(46) Yan, J.; Ding, Y.; Hu, C.; Cheng, H.; Chen, N.; Feng, Z.; Zhang, Z.; Qu, L. *J. Mater. Chem. A* **2014,** *2*, 16786.

(47) Vickery, J. L.; Patil, A. J.; Mann, S. *Adv. Mater.* **2009,** *21*, 2180.

(48) Fang, Q.; Shen, Y.; Chen, B. *Chem. Eng. J.* **2015,** *264*, 753.

(49) Xu, Y.; Shi, G.; Duan, X. *Acc. Chem. Res.* **2015,** *48*, 1666.

(50) Xu, Y.; Sheng, K.; Li, C.; Shi, G. *ACS Nano* **2010,** *4*, 4324.

(51) Xu, Y.; Lin, Z.; Huang, X.; Liu, Y.; Huang, Y.; Duan, X. *ACS Nano* **2013,** *7*, 4042.

(52) Xie, X.; Zhou, Y.; Bi, H.; Yin, K.; Wan, S.; Sun, L. *Sci. Rep.* **2013,** *3*.

(53) Chang, H.; Qin, J.; Xiao, P.; Yang, Y.; Zhang, T.; Ma, Y.; Huang, Y.; Chen, Y. *Adv. Mater.* **2016,** *28*, 3504.

(54) Sudeep, P. M.; Narayanan, T. N.; Ganesan, A.; Shaijumon, M. M.; Yang, H.; Ozden, S.; Patra, P. K.; Pasquali, M.; Vajtai, R.; Ganguli, S.; Roy, A. K.; Anantharaman, M. R.; Ajayan, P. M. *ACS Nano* **2013,** *7*, 7034.

(55) Chen, K.; Chen, L.; Chen, Y.; Bai, H.; Li, L. *J. Mater. Chem.* **2012,** *22*, 20968.

(56) Navalon, S.; Dhakshinamoorthy, A.; Alvaro, M.; Antonietti, M.; Garcia, H. *Chem. Soc. Rev.* **2017,** *46*, 4501.

(57) Tong, X.; Wei, Q.; Zhan, X.; Zhang, G.; Sun, S. *Catalysts* **2017,** *7*.

(58) Zhang, J.; Qu, L.; Shi, G.; Liu, J.; Chen, J.; Dai, L. *Angew. Chem. Int. Ed.* **2016,** *55*, 2230.

(59) Guo, D.; Shibuya, R.; Akiba, C.; Saji, S.; Kondo, T.; Nakamura, J. *Science* **2016,** *351*), 361.

(60) Dai, L.; Xue, Y.; Qu, L.; Choi, H.-J.; Baek, J.-B. *Chem. Rev.* **2015,** *115*, 4823.

(61) Ma, Y.; Sun, L.; Huang, W.; Zhang, L.; Zhao, J.; Fan, Q.; Huang, W. *J. Phys. Chem. C* **2011,** *115*, 24592.

(62) Zhao, Y.; Hu, C.; Hu, Y.; Cheng, H.; Shi, G.; Qu, L. *Angew. Chem. Int. Ed.* **2012,** *51*, 11371.

(63) Zhou, X.; Bai, Z.; Wu, M.; Qiao, J.; Chen, Z. *J. Mater. Chem. A* **2015,** *3*, 3343.

(64) Yang, X.; Liu, A.; Zhao, Y.; Lu, H.; Zhang, Y.; Wei, W.; Li, Y.; Liu, S. *ACS Appl. Mater. Interfaces* **2015,** *7*, 23731.

(65) Zhang, J.; Zhao, Z.; Xia, Z.; Dai, L. *Nat. Nanotech.* **2015,** *10*, 444.

(66) Xu, C.; Su, Y.; Liu, D.; He, X. *Phys. Chem. Chem. Phys.* **2015,** *17*, 25440.

(67) Su, Y.; Zhang, Y.; Zhuang, X.; Li, S.; Wu, D.; Zhang, F.; Feng, X. *Carbon* **2013,** *62*, 296.

(68) Wu, X.; Xie, Z.; Sun, M.; Lei, T.; Zuo, Z.; Xie, X.; Liang, Y.; Huang, Q. *Rsc Adv.* **2016,** *6*, 90384.

(69) Li, Y.; Yang, J.; Huang, J.; Zhou, Y.; Xu, K.; Zhao, N.; Cheng, X. *Carbon* **2017,** *122*, 237.

(70) Chabu, J. M.; Wang, L.; Tang, F.-Y.; Zeng, K.; Sheng, J.; Walle, M. D.; Deng, L.; Liu, Y.-N. *Chemelectrochem* **2017,** *4*, 1885.

(71) Ahmed, M. S.; Kim, Y.-B. *Sci. Rep.* **2017,** *7*.

(72) Vineesh, T. V.; Alwarappan, S.; Narayanan, T. N. *Nanoscale* **2015,** *7*, 6504.

(73) Tian, J.; Ning, R.; Liu, Q.; Asiri, A. M.; Al-Youbi, A. O.; Sun, X. *ACS Appl. Mater. Interfaces* **2014,** *6*, 1011.

(74) Patil, I. M.; Lokanathan, M.; Kakade, B. *J. Mater. Chem. A* **2016,** *4*, 4506.

(75) Zhang, L. Y.; Liu, Z.; Xu, B.; Liu, H. *Int. J. Hydrogen Energy* **2017,** *42*, 28278.

(76) Xu, Y.; Kraft, M.; Xu, R. *Chem. Soc. Rev.* **2016,** *45*, 3039.

(77) Wang, X.; Maeda, K.; Thomas, A.; Takanabe, K.; Xin, G.; Carlsson, J. M.; Domen, K.; Antonietti, M. *Nat. Mat.* **2009,** *8*, 76.

(78) Ge, L.; Han, C. *Appl. Catal. B-Environ.* **2012,** *117*, 268.

(79) Min, S.; Lu, G. *J. Phys. Chem. C* **2012,** *116*, 19644.

(80) Ge, L.; Han, C.; Xiao, X.; Guo, L.; Li, Y. *Mater. Res. Bull.* **2013,** *48*, 3919.

(81) Liu, J.; Liu, Y.; Liu, N.; Han, Y.; Zhang, X.; Huang, H.; Lifshitz, Y.; Lee, S.-T.; Zhong, J.; Kang, Z. *Science* **2015,** *347*, 970.

(82) Liang, Q.; Li, Zhi; Yu X.; Huang Z.; Kang F.; Yang Q. *Adv. Mater.* **2015,** *27*, 4634.

(83) Lu, Y.; Ma, B.; Yang, Y.; Huang, E.; Ge, Z.; Zhang, T.; Zhang, S.; Li, L.; Guan, N.; Ma, Y.; Chen, Y. *Nano Res.* **2017,** *10* (5), 1662-1672.

(84) Tian, Y.; Ye, Y.; Wang, X.; Peng, S.; Wei, Z.; Zhang, X.; Liu, W. *Appl. Catal. a-Gen* **2017,** *529*, 127.

(85) Gangadharan, P. K.; Unni, S. M.; Kumar, N.; Ghosh, P.; Kurungot, S. *Chemelectrochem* **2017,** *4*, 2643.

(86) Tong, Z.; Yang, D.; Shi, J.; Nan, Y.; Sun, Y.; Jiang, Z. *ACS Appl. Mater. Interfaces* **2015,** *7*, 25693.

TOC

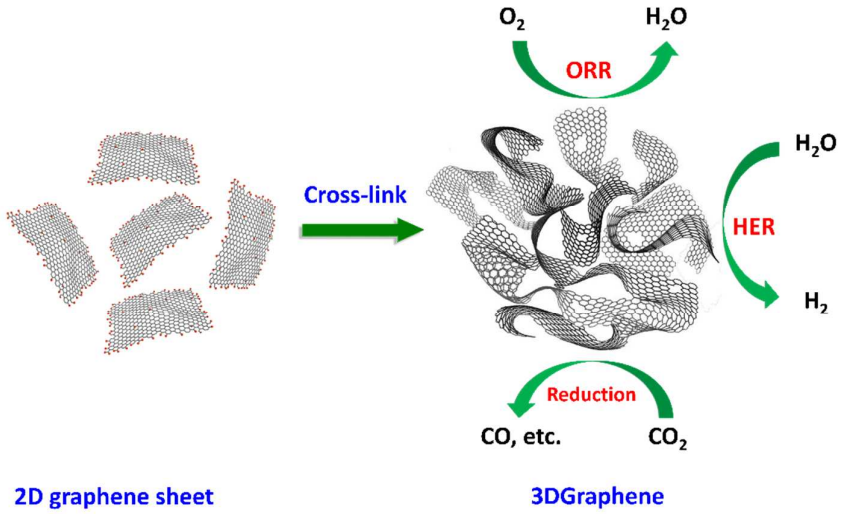

2D graphene sheets need to be built as a 3D cross-linked structure in the bulk state before its many exciting properties could be achieved for bulk applications, including that for metal-free redox catalysis. Thus, the fabrication of such 3D cross-linked graphene materials and their redox catalytic application are reviewed in this Perspective.